



ELSEVIER

Available online at www.sciencedirect.com

SCIENCE @ DIRECT®

JOURNAL OF
GEODYNAMICS

Journal of Geodynamics 37 (2004) 337–359

www.elsevier.com/locate/jog

Exhumed Himalayan-type syntaxis in the Grenville orogen, northeastern Laurentia

Alexander E. Gates^{a,*}, David W. Valentino^b, Jeffrey R. Chiarenzelli^c,
Gary S. Solar^d, Michael A. Hamilton^{e,1}

^a*Department of Earth and Environmental Sciences, Rutgers University, Newark, NJ 07102, USA*

^b*Department of Earth Sciences, State University of New York at Oswego, Oswego, NY 13126, USA*

^c*Department of Geology, State University of New York at Potsdam, Potsdam, NY 13676, USA*

^d*Department of Earth Sciences, State University of New York, College at Buffalo, Buffalo, NY, 14222, USA*

^e*Geological Survey Canada, 601 Booth St., Ottawa, Ontario, Canada K1A 0E8*

Abstract

A deep-seated analog of the syntaxis developed in the Tibetan Plateau occurs in the Grenville Orogen of eastern Laurentia. During the final assembly of Rodinia, Amazonia collided with Laurentia and produced a series of large, conjugate, transcurrent, shear systems and pervasive strike-slip deformation that overprinted compressional structures related to the Ottawa Orogeny (the last orogenic phase of what is considered Grenvillian). A northeast-striking dextral system at least 35-km wide developed in the Reading Prong of New York (locally known as the Hudson Highlands), New Jersey, and Pennsylvania. U-Pb SHRIMP zircon geochronology and Ar/Ar thermochronology on the lowest grade cataclasites constrain the age of movement between 1008 and 876 Ma. A 60-km-wide, east-west striking, sinistral shear system developed across the central Adirondack Highlands. This system overprints rocks with granulite-facies metamorphic assemblages containing ca. 1050 Ma metamorphic zircons and is cut by a swarm of 950 Ma leucogranites. The timing, geometric relationships, and shear sense of the Adirondacks and Reading Prong shear systems suggest a conjugate system within a syntaxis with bulk compression directed ENE–WSW. This tectonic scenario invokes a component of strike-parallel deformation during the Ottawa Orogeny and provides a kinematic mechanism for an otherwise enigmatic, synchronous, late (ca. 930 Ma) extensional event including the Carthage–Colton mylonite zone in the northwest Adirondacks and Canada.

© 2004 Elsevier Ltd. All rights reserved.

* Corresponding author.

E-mail address: agates@andromeda.rutgers.edu (A.E. Gates).

¹ Current address: 605 Island Park Cres., Ottawa, Ontario, Canada K1Y 3P4.

1. Introduction

Dewey and Burke (1973) and Windley (1986) proposed an analogy between the deep structure of Himalayas and the Grenville Province based upon the intensity of tectonism. Tapponnier and Molnar (1977) proposed that the rigid indentation of India formed a syntaxis (abrupt bend in the general attitude of the orogen) containing conjugate strike-slip faults in the Eurasian continent during the Himalayan Orogeny. Extensive northeast-trending sinistral, transcurrent shear systems accommodate tectonic escape (Tapponnier et al., 1982) in China and southeast Asia. These systems record hundreds to thousands of kilometers of offset over tens of millions of years. However, there are smaller, northwest-striking, dextral systems that have been synchronously active with the sinistral zones within a much smaller area to the north of the suture zone. They form the conjugate pairs to the larger zones of tectonic escape within this syntaxis.

The Himalayan syntaxis is still active and recent work suggests a direct correlation between the observed crustal structures and the stress field in the mantle (Holt, 2000). Described here is what the roots of the Himalayan syntaxis might look like through a possible analog in the Grenville orogen in the northeastern United States (Fig. 1). This analysis is based on new data on the tectonics, kinematics, geometry and supporting geothermochronology of large, apparently conjugate, ductile fault systems in New York, New Jersey and eastern Pennsylvania, and provides a testable kinematic model for the terminal stages of what is considered Grenvillian (Ottawan Orogeny; McLelland et al., 2001) in northeastern Laurentia, and final assembly of the Rodinian supercontinent.

2. Grenville orogen

Grenville massifs in the northeastern United States form a series of unconnected inliers along the Appalachians (Fig. 1). Because of the great spacing and high degree of tectonism of various ages, correlations among the massifs are difficult. Paramount among the similarities is widespread deformation and metamorphism to granulite-facies conditions at about 1.0 Ga. The oldest ages reported from these massifs are also consistently ca. 1.2–1.3 Ga (Mose, 1982). Another point of commonality appears to be the intrusion of vast volumes of a-type granitoids prior to Ottawan deformation into older supracrustal rocks of varied character (McLelland and Isachsen, 1986). The Grenville Province forms one of the longest and most deeply exhumed areas of continental crust on Earth, extending from Scandinavia, through eastern Canada and inliers in the Appalachian chain, to Texas and Mexico, and perhaps beyond. By inference it exposes the deep crustal roots of an ancient mountain range of immense portions, and records the assembly of one of the Earth's few recognized supercontinents, Rodinia. Consequently the Ottawan Orogeny (ca. 1070–1000 Ma) is often cited as a classic example of continent-continent collision and compressive thickening of the crust, with invocation of the Himalayas as a modern tectonic reference frame (Dewey and Burke, 1973; Windley, 1986; McLelland et al., 2001). However, refinement and testing of such analogies must address many important components of the orogeny. One of the most significant components in the Himalayas, is the massive amount of strike-slip faulting expressed in tectonic escape and the syntaxis (Tapponnier and Molnar, 1977). Whereas compressive tectonics is universally documented in the Grenville orogen, few workers have recognized analogous, large-scale, orogen-parallel deformation (cf. Baer, 1977).

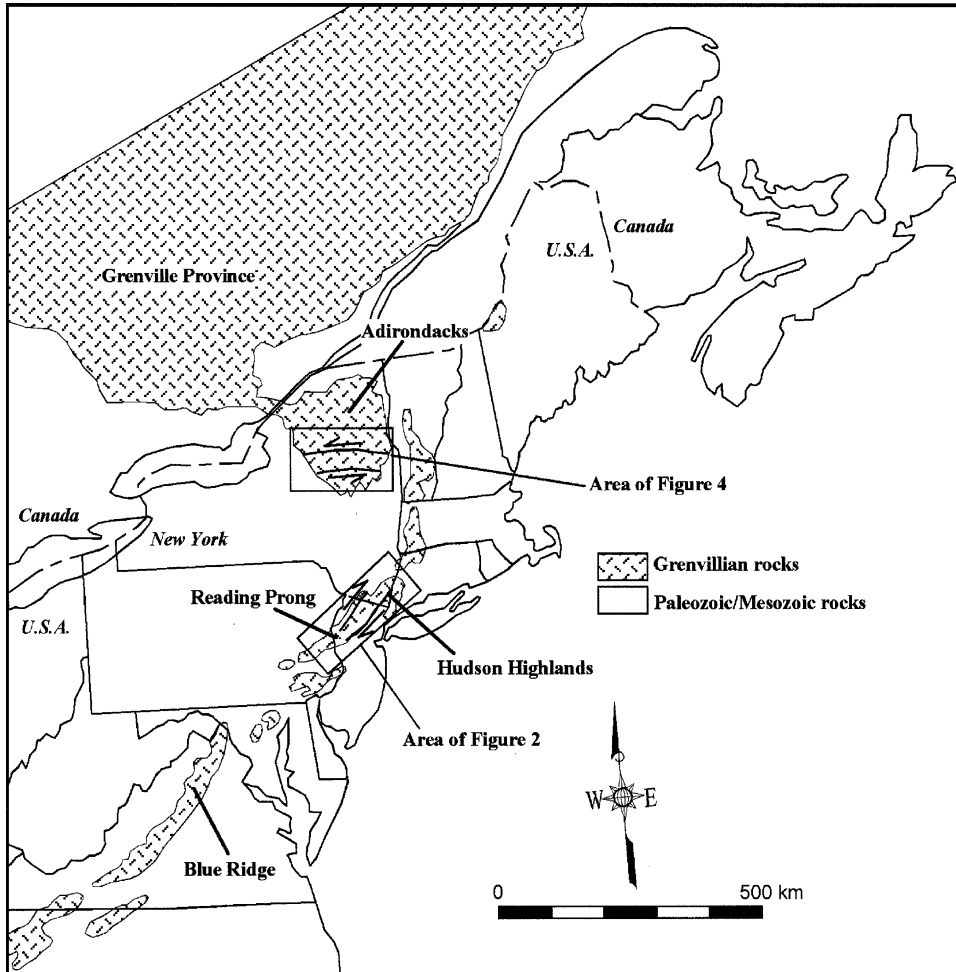


Fig. 1. Regional map of exposed Grenville basement massifs in northeastern North America showing the locations of the Hudson Highlands and Adirondack Mountains.

3. Reading Prong and Hudson Highlands

Gates (1995) and Gates and Costa (1998) proposed a post-peak, Grenville, dextral strike-slip event in the Reading Prong (Fig. 2). Several regionally extensive fault zones, Ramapo (NY-NJ), Reservoir (NJ), and Morgan Hill (PA), exhibit mylonites and cataclasites with consistent, dextral, strike-slip, kinematic indicators (Gates, 1995). These nearly vertical northeast-trending zones overprint slightly earlier northwest-directed fold nappes and accompanying peak granulite-facies metamorphism and anatexis (Gates, 1999). In contrast to the vertical shear zones, the earlier fabric is shallowly dipping in the western Hudson Highlands. The dextral mylonites are rarely crossed by small west-northwest-trending sinistral zones. The dextral-shearing event was hypothesized to result from tectonic escape propagating from a collision to the north (Gates, 1999). Gates et al. (1999) found that the dextral shearing was not restricted to a few widely spaced zones, but instead

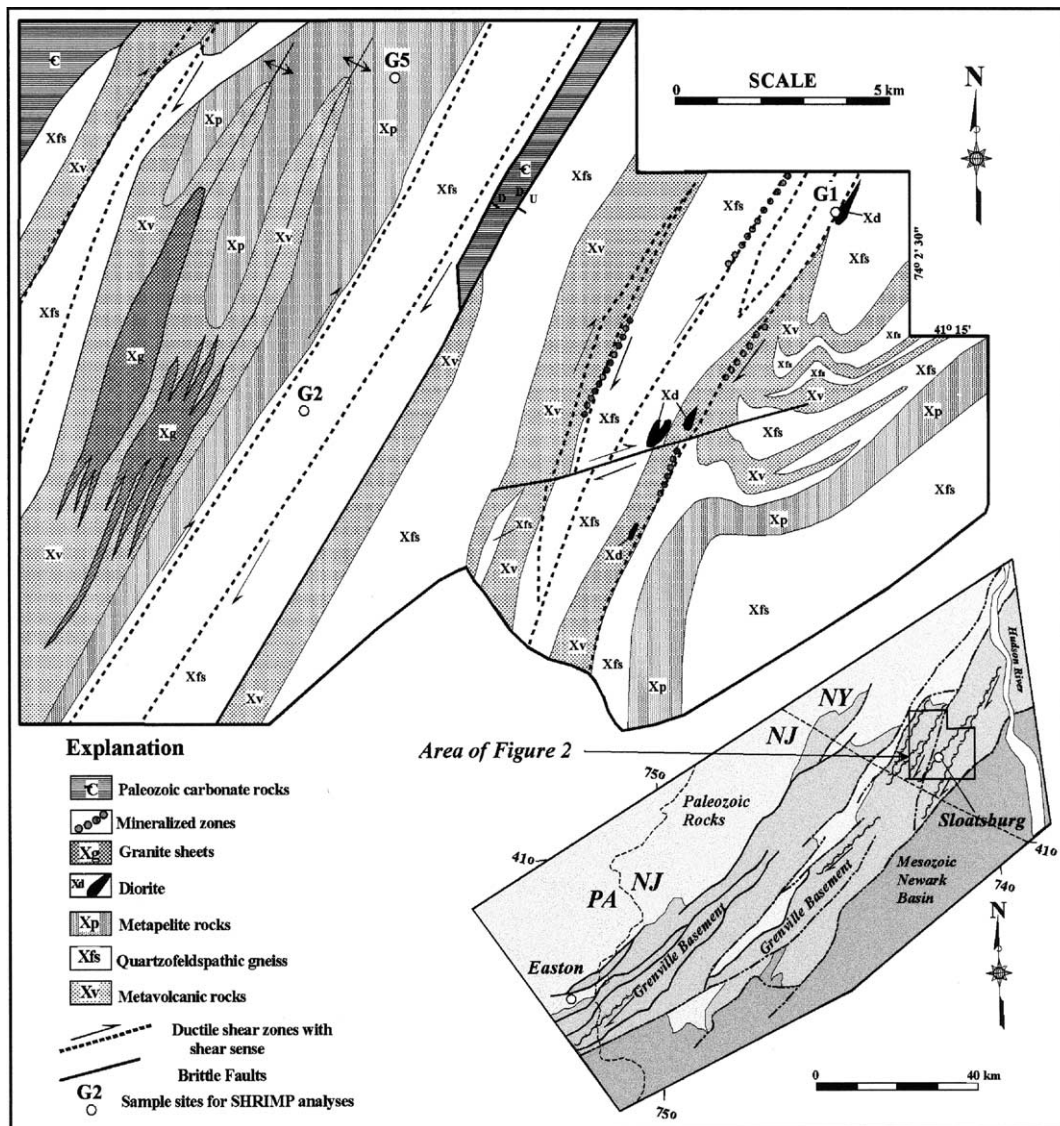


Fig. 2. Geologic map of the New York Hudson Highlands showing the distribution of dextral shear zones and locations where samples were collected for U-Pb SHRIMP analyses (Fig. 7). Inset map shows the Reading Prong and the regional distribution of dextral shear zones.

formed a regionally pervasive system. A belt of anastomosing shear zones at least 35-km wide is found in the central Highlands of New York (western Hudson Highlands) and New Jersey (Fig. 2).

These shear zones are primarily 1- to 5-km wide bands of amphibolite and granulite facies mylonite with foliation ranging from 030 to 045°, and lineations plunging 8–20° northeast. Although no offset units are observed, several drag folds with amplitudes up to 5 km have been identified. Kinematic indicators within the mylonites include S-C fabric, rotated σ -type porphyroclasts, shear bands, and isoclinal intrafolial folds, all with a consistent dextral sense (Fig. 3).

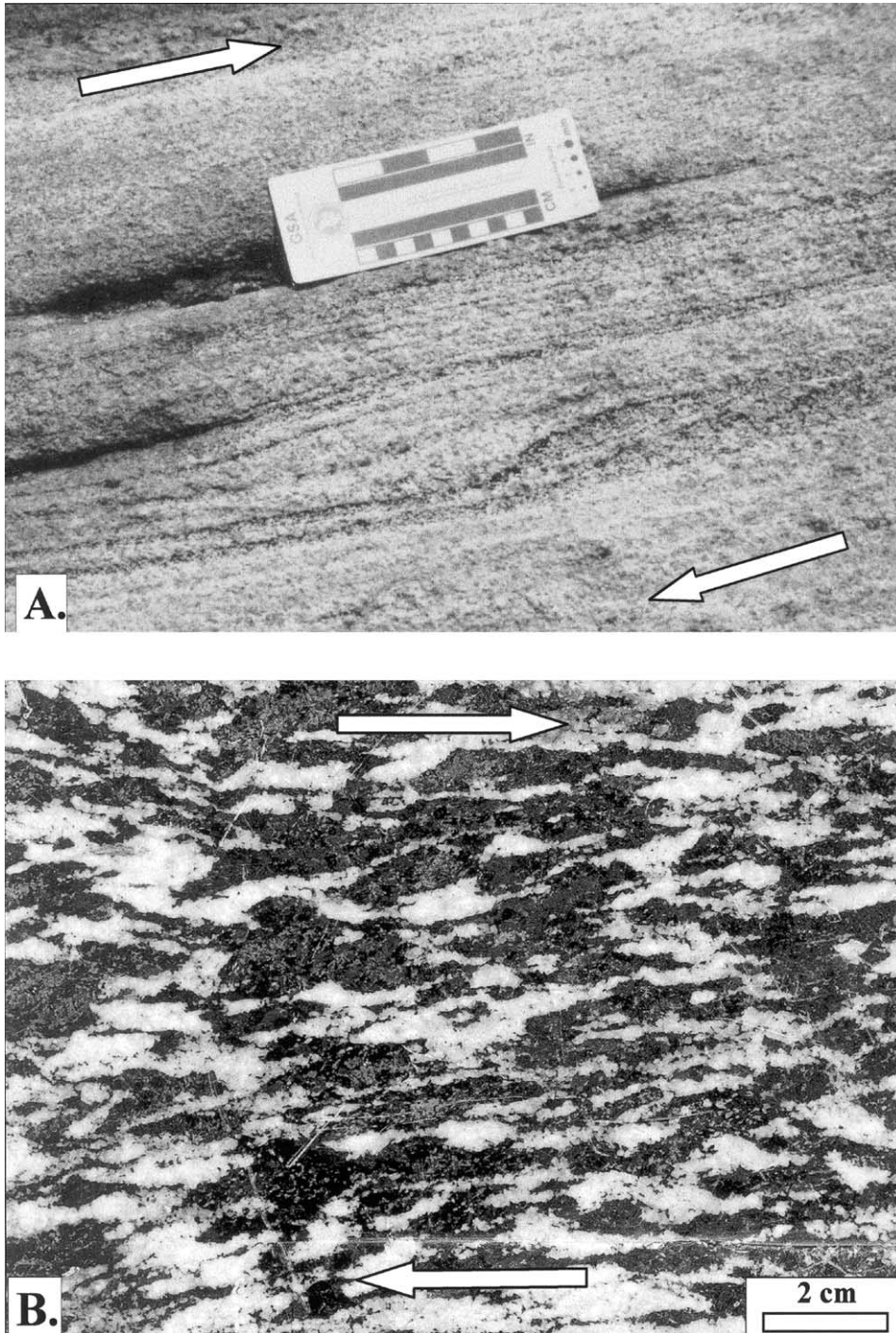


Fig. 3. Examples of shear-sense indicators from the Hudson Highlands. (A) Recrystallized asymmetric trails developed on a quartz-feldspar aggregate from sheared quartzofeldspathic gneiss; and (B) Type-I S-C fabrics developed in sheared diorite.

Sheath folds and shear boudins occur along the margins. Transpressional features like en echelon folds and synchronous small reverse faults are also present. Axial traces of en echelon folds trend roughly north-south, an orientation that is mechanically consistent with concurrent formation within the dextral mylonite zones. The folds were variably rotated into parallelism with the transcurrent zones. Mineral assemblages within the mylonites are indicative of lower granulite facies conditions during deformation. A few of the larger shear zones remained active to lower temperatures. They exhibit brittle deformation and mineralization with chlorite, biotite, and amphibole including tremolite, actinolite, and hastingsite (Gates, 1995). In several cases, dilational fractures up to 10-km long opened up along the zone margins and were mineralized with magnetite, sulfides, salite, and other gangue minerals, depending upon the country rock (Gates, 1999). Fracture zones in marble are dominated by calcite, by quartz in quartzofeldspathic gneiss, and by pyrite in sulfide-bearing rocks. Locally, the mylonite zones were later intruded by pegmatites and granites.

4. Adirondack Highlands

In contrast to the overwhelming northeast trends throughout most of the Grenville Province, the structural grain of the south-central Adirondack Highlands is generally east-west (Figs. 4 and 5).

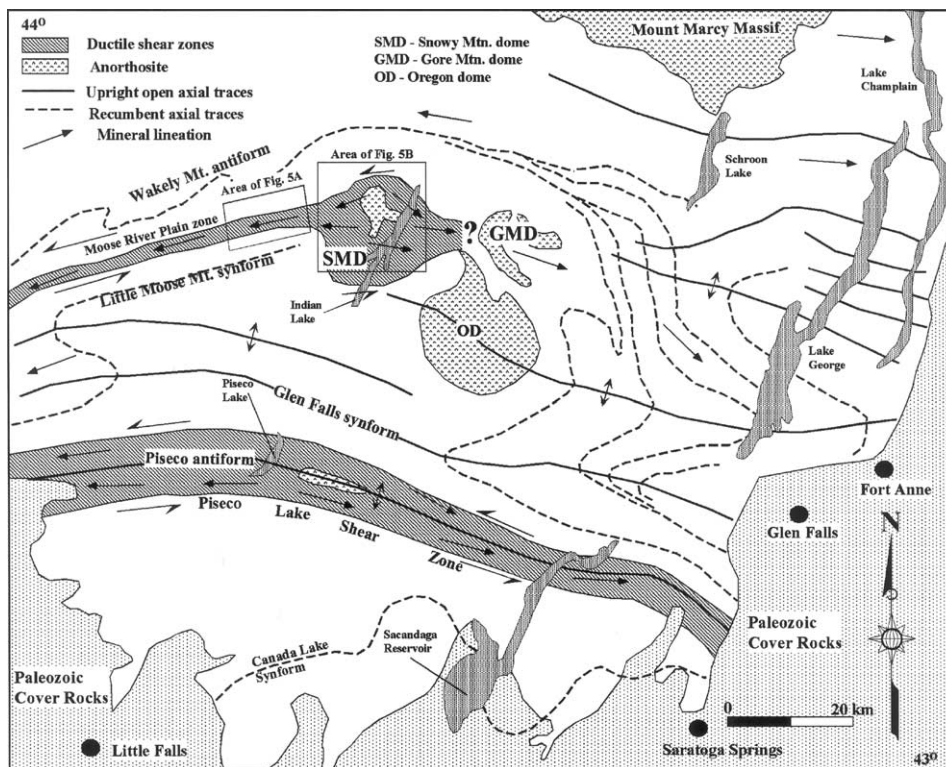


Fig. 4. Geologic map of the southern Adirondacks showing the major ductile shear zones, folds and domes. Locations of maps for Fig. 5 are shown.

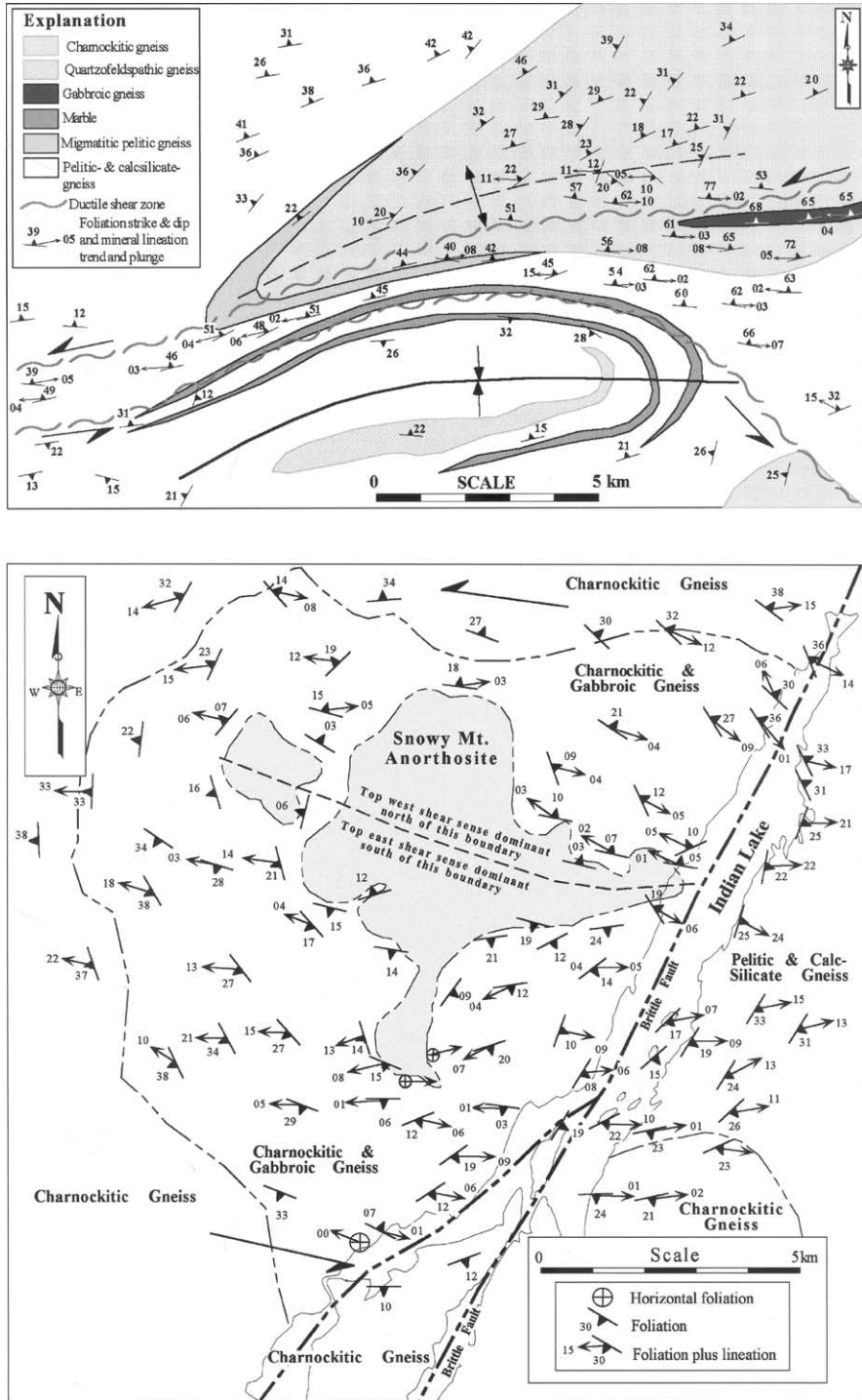


Fig. 5. Detailed geologic maps of study areas in the Adirondack Mountains with locations shown in Fig. 4. (A) Geologic map of the Moose River plain shear zone, and (B) Geologic map of the Snowy Mountain dome.

This broad zone (>60-km wide) displays a nearly universal parallelism of lithologic and intrusive contacts, fold axes, compositional layering, foliation, subhorizontal lineations and an anastomosing system of mylonite zones. Several large (>20-km across) structural domes cored by rheologically rigid anorthosite lie within the zone. Kinematic investigations indicate that this zone is dominated by sinistral transpression (Chiarenzelli et al., 2000). There are a number of large-scale features (drag folds and rotated megacrysts) which are consistent with the abundant meso- and micro-scale kinematic indicators. Kinematic indicators include S-C fabrics, shear bands, and rotated porphyroclasts. The broad zone is bounded by shear zones that traverse portions of the southern Adirondacks (Fig. 4). The structure of the south-central Adirondacks has been interpreted as the consequence of transpressional modification of earlier crustal-scale recumbent folds analogous to those exposed in the Adirondack Lowlands (Chiarenzelli et al., 2000). Widespread granulite-facies mineral assemblages within substantial volumes of supracrustal rocks are consistent with compressional tectonics; however, the southernmost bounding shear zone (the Piseco Lake shear zone) has mineral assemblages that indicate deformation outlasted high-grade conditions.

4.1. Piseco Lake shear zone

A broad east-west zone (10–15 km wide) of L–S and L>S tectonite crosses the southern Adirondacks (Fig. 4). The Piseco Lake shear zone (PLSZ) coincides with the Piseco antiform (Glennie, 1973; McLelland, 1984; Wiener et al., 1984), but extends well beyond the core of the antiform (Fig. 4). Throughout the PLSZ, rocks of mostly granitic composition contain intense foliation and lineation. McLelland (1984) described the formation of ribbon lineations in these tectonites.

4.1.1. Deformation fabrics

The PLSZ rocks contain penetrative foliation and lineation defined by dynamically recrystallized quartz, K-feldspar and plagioclase, and alignment of phyllosilicates such as muscovite, biotite and locally chlorite. Most rocks within the zone consist of fine-grained polygonal aggregates of these minerals; however, locally there are relict orthoclase megacrysts (2–6 cm) preserved in lower strain domains. Foliation within the PLSZ defines an upright antiform (Glennie, 1973; Wiener et al., 1984) with a subhorizontal hinge that trends approximately 110° . Foliation on the antiform limbs dips moderately to steeply both north and south. Lineations are pervasive in these rocks and are defined by dynamically recrystallized ribbons and rods of quartz, K-feldspar, plagioclase and streaks of chlorite, biotite, magnetite and muscovite. The plunges of these lineations are consistently subhorizontal. In the crest of the antiform, foliation is not as well developed as in the limbs, but lineations defined by mineral-rods, mineral rod aggregates, and mineral ribbons are pervasive. Lineations in the PLSZ are intensely developed, and in many places the linear fabric is dominant over the planar fabric ($L \gg S$) (Fig. 6A) with grain-shape aspect ratios upward of 60:1.

The penetrative foliation and lineation within the PLSZ is associated with diagnostic metamorphic minerals such as muscovite, biotite and chlorite, indicative of greenschist-facies conditions. However, the metamorphic history of the rocks within the PLSZ is complex, with an early granulite-facies mineral assemblage (McLelland, 1984), overprinted by the greenschist-facies assemblages (Chiarenzelli et al., 2000).

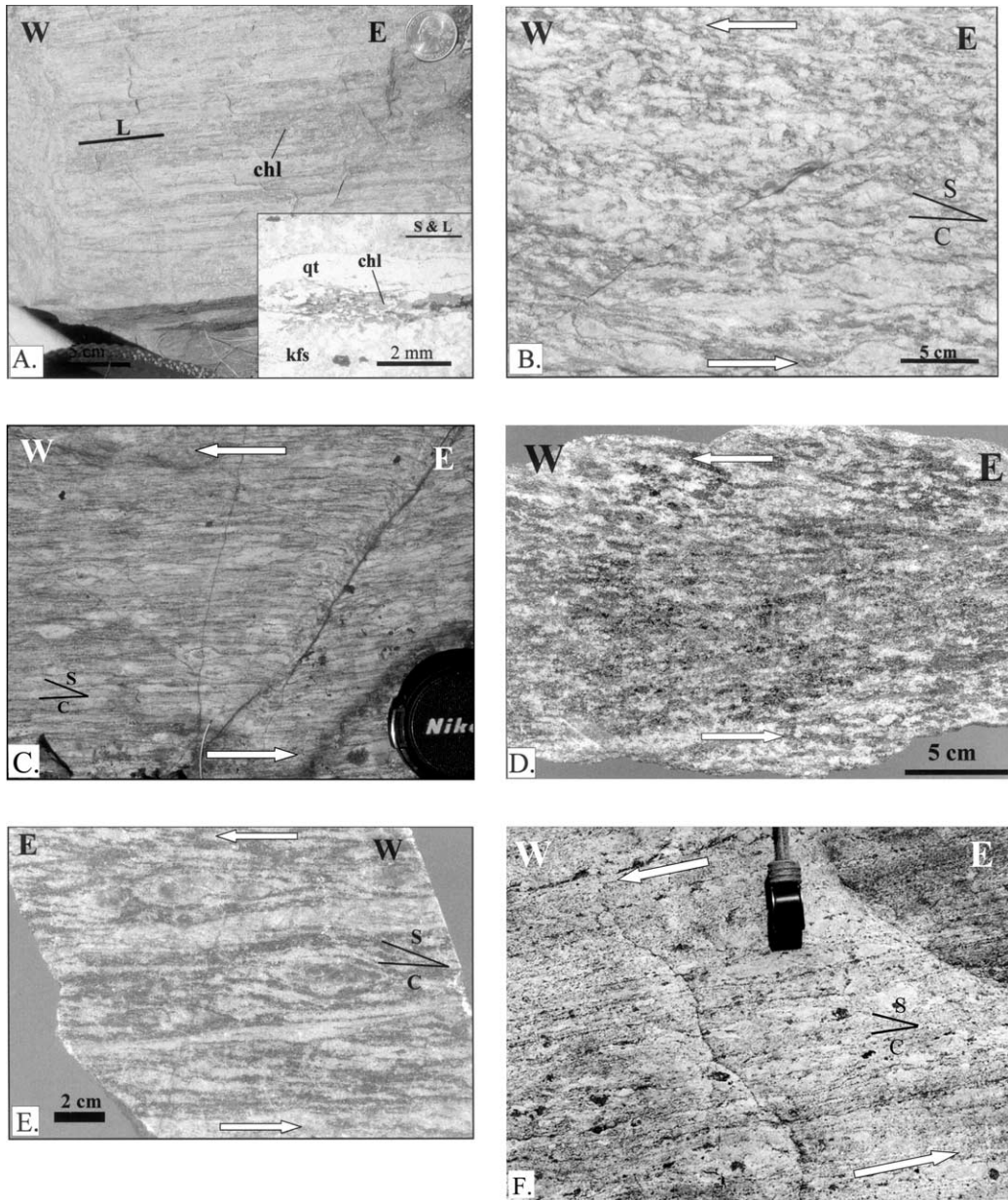


Fig. 6. Examples of structures and microstructures from the south central Adirondacks: (A) L-S mylonite from the Piseco Lake shear zone with domains of chlorite defining the deformation fabric (photomicrograph inset shows the fabric forming chlorite); (B) Sinistral type I S-C fabrics developed in megacrystic granite from the northern part of the Piseco Lake shear zone; (C) Sinistral σ -clasts of plagioclase feldspar from the southern part of the Piseco Lake shear zone; (D) Small sinistral high-strain zone developed in gabbroic gneiss from the Moose River Plain shear zone; (E) Type I S-C fabric in charnockitic gneiss from the southern flank of the Snowy Mountain dome showing sinistral shear sense; and (F) Type I S-C fabric in pelitic gneiss from the northwestern flank of the Snowy Mountain dome showing sinistral shear sense.

4.1.2. Kinematic analysis

McLelland (1984) suggested that the Piseco dome evolved in the constrictional part of a regional west-directed thrust but did not perform a detailed kinematic analysis. Shear-sense indicators in the PLSZ include Type I S-C fabrics (Lister and Snoke, 1984), σ - and δ -porphyroclasts (Simpson and Schmid, 1983; Passchier and Simpson, 1986) of K-feldspar, and biotite- and muscovite-fish (Figs. 6B and 6C). These kinematic indicators reveal a consistent sinistral-shear sense on both the north and south limbs of the Piseco antiform.

4.2. Moose River Plain shear zone and Snowy Mountain dome

A zone of intensely sheared rocks (Figs. 4 and 5A) extends east-west through the Moose River Plain, west-central Adirondacks and is herein named the Moose River Plain shear zone (MRPSZ). This shear zone occurs between the Wakely Mountain antiform and Little Moose Mountain synform (Wiener et al., 1984), and it experienced sinistral shearing under granulite-facies conditions. The eastward trace of the MRPSZ intersects and is deflected around the north side of the anorthosite-cored Snowy Mountain dome (DeWaard and Romey, 1969). East of the Snowy Mountain dome, the MRPSZ is yet to be delineated.

4.2.1. Deformation fabrics in the Moose River Plain shear zone

Penetrative foliation occurs along a narrow belt (~2 km wide) that defines the MRPSZ. The foliation generally strikes 270° and dips moderately to steeply north (Fig. 5A). It is defined by metamorphic mineral assemblages characteristic of granulite-facies conditions. Sheared charnockitic gneiss contains the assemblage plagioclase-clinopyroxene-hypersthene, pelitic gneiss contains biotite-K-feldspar-sillimanite-garnet, and gabbroic-gneiss contains augite-hypersthene-garnet-plagioclase. Local migmatite in the sheared charnockitic gneiss suggests anatexis during deformation. Within granitic and charnockitic gneisses, foliation is defined by planar aggregates of recrystallized feldspars and quartz. Foliation in pelitic gneiss is defined by recrystallized quartz and K-feldspar and parallel alignment of biotite and sillimanite. Mineral-elongation lineations are defined by linear aggregates of feldspar, pyroxene and garnet in charnokite and biotite and sillimanite in pelitic gneiss. The foliation and lineation in the gabbroic gneiss is mostly defined by alternating planar aggregates of plagioclase and pyroxenes. The eastern limit of the MRPSZ is structurally continuous with the penetrative foliation that mantles the Snowy Mountain dome (DeWaard and Romey, 1969).

4.2.1.1. Kinematic analysis. The zone of deformed rocks in the Moose River Plain region was interpreted as the result of shearing between the lower and upper limb of the Wakely Mountain antiform and Little Moose Mountain synform (Wiener et al., 1984). Consistent subhorizontal mineral lineations throughout the Moose River Plain shear zone are indicative of a subhorizontal transport direction. Kinematic indicators throughout the shear zone are consistent with a left-lateral shear couple. Kinematic indicators include σ - and δ -type porphyroclasts (Simpson and Schmid, 1983; Passchier and Simpson, 1986) in pelitic and granitic gneiss, type-I S-C fabrics in charnockitic gneiss, asymmetric foliation boudins often associated with local migmatite, and fish-structures comprised of broken garnet crystals, and small high-strain zones (Fig. 6D). Locally the foliation is deflected at the margins of the MRPSZ consistent with left-lateral drag folds (Fig. 5A).

4.2.2. Deformation fabrics in the Snowy Mountain dome

Large (15–20-km across) structural domes cored by anorthosite in the Adirondack Highlands are interpreted to have resulted from fold interference (McLelland and Isachsen, 1986) (Figs. 4 and 5B). The Snowy Mountain dome is composed of a suite of anorthosite-mangerite-charnockite-granite (AMCG suite) rocks with anorthosite in the core (DeWaard and Romey, 1969). The eastern extent of the MRPSZ foliation is structurally continuous with penetrative-deformation fabrics that wrap around the Snowy Mountain dome. The core of the dome is composed of megacrystic anorthosite with crystals up to 20-cm. Anorthosite grades outward into gabbroic and then charnockitic gneiss forming a concentric compositional zonation (DeWaard and Romey, 1969). Although the central anorthosite is relatively undeformed, the margins contain a well-developed foliation defined by dynamically recrystallized plagioclase. The transition from anorthosite to gabbroic gneiss is marked by stronger deformation fabrics away from the dome core. These fabrics are penetrative farther outward on the flanks of the dome in the charnockitic gneiss (Fig. 5B). Only relict plagioclase crystals are present in the charnockitic gneiss suggesting a plutonic origin. Most of the unit consists of planar and linear aggregates of recrystallized plagioclase and anhedral, broken grains of clinopyroxene and hypersthene. Poles to foliation reveal that the dome has a dominant northwest-southeast-trending axis. Although foliation varies around the dome, the variation in lineation trend is about 30°, with most mineral lineations trend east–west, parallel to those in the MRPSZ, which is located due west of the dome.

4.2.2.1. Kinematic analysis. Two classes of shear-sense indicators were observed in the MRPSZ including σ - and δ -porphyroclasts (Passchier and Simpson, 1986), and type-I S-C fabrics (Lister and Snoke, 1984). Shear-sense indicators from the southern flank of the dome show top-to-the-east bulk shear (Fig. 6E), whereas the northwestern flank shows top-to-the-west shear (Fig. 6F). On the northwest side of the dome, where foliation dips moderately westward, the shear sense is locally dip-slip normal. On this basis, the dome can be divided into two domains as shown on Fig. 5B. These shear domains form the eastern continuation of the sinistral MRPSZ deflected around the massif anorthosite that cores the dome. The axial obliquity of the dome with respect to the general east-west shear along the MRPSZ is consistent with large-scale rotation of the dome in a sinistral-shear couple, and the formation of the dome by sinistral transpression.

5. Geochronology/Thermochronology

Isotopic analyses of zircons from three lithologies in the western Hudson Highlands were carried out using the Sensitive High-Resolution Ion Microprobe (SHRIMP II) at the Geological Survey of Canada in Ottawa. Initial inspection using cathodoluminescence of many of the zircons revealed sufficient internal growth complexities (e.g., irregular cores, overgrowths) that in situ SHRIMP methods were required to obtain unambiguous U-Pb ages and thereby constrain the timing of igneous activity, regional metamorphism, and dextral shearing. Protocols, analytical procedures and data reduction methods for SHRIMP geochronology summarized in this paper generally followed those outlined by Stern (1997), while specific operating conditions for this analytical session were similar to those described by Hamilton et al. (2003). Data for these analyses, as well as further instrumental details, are presented in Table 1.

The samples analyzed include a semi-pelitic gneiss (G5) within the metasedimentary unit, a feldspathic gneiss (G2) that lies within the large dextral Indian Hill shear zone and the small Lake Tiorati diorite that cross-cuts regionally metamorphosed rocks but which subsequently underwent dextral shearing (G1) (Gates et al., 1999) (Fig. 2). Uncertainties in isotopic ratios and ages presented in Table 1, and as error ellipses in Fig. 7, are presented at the 1σ level. Calculated, weighted, mean ages reported in the text, however, are given at the 2σ level.

Zircons from the semi-pelitic gneiss are small, rounded to subrounded, and typically show strong internal zonation with distinct, often irregular, cores and thick homogeneous rims (Fig. 7A). We interpret the cores of these zircons to be detrital in origin and the structureless, low Th/U (mostly <0.06) rims to be associated with an episode of regional metamorphism (Table 1). Zircon cores show a spectrum of ages from roughly 1200–2000 Ma, whereas the rims yield a narrow range of ages from 1000–1030 Ma, the bulk of these analyses clustering between approximately 1005–1010 Ma (Fig. 7B). A weighted mean calculated for the most precise, clustered, concordant, spot analyses on metamorphic rims best constrains the time of high-grade metamorphism in sample G5 at 1007 ± 4 Ma ($\pm 2\sigma$, $N = 10$, MSWD = 1.3).

Sample G2 is quartzofeldspathic gneiss which is interpreted to be a metavolcaniclastic rock (Gates et al., 1999). It contains generally elongate zircons with broad, oscillatory-zoned cores, locally with structureless, unzoned rims having slightly rounded external grain boundaries (Fig. 7C). Analyses of the cores and rims produced two clusters of concordant ages (Fig. 7D). The cores range rather broadly in $^{207}\text{Pb}/^{206}\text{Pb}$ age from ca. 1160–1230 Ma, whereas the rim ages range from approximately 1010–1060 Ma. We interpret ages from the zoned cores to represent the timing of crystallization of the igneous protolith(s) of this unit. These are dominated by grain-core and mantle domains whose ages appear in part to be coeval with arc/back-arc magmatic (and metamorphic) rocks of Elzevirian age from the Central Metasedimentary Belt of southern Quebec, eastern Ontario and northern New York state (McLelland et al., 1996; Rivers, 1997; Wasteneys et al., 1999). At present, the best estimate of the timing of late, overprinting metamorphism recorded in quartzofeldspathic gneiss G2 comes from only three robust rim analyses, all characterized by low Th/U (<0.12), which suggest an age of approximately 1012 Ma (Fig. 7D). We conclude that the development of these thin metamorphic zircon rims was directly associated with the Indian Hill shear zone.

Zircons recovered from the Lake Tiorati diorite body are moderately sized (~ 150 – 250 microns), subhedral to anhedral fragments likely comminuted from larger grains during crushing. Cathodoluminescence studies reveal that these zircons possess only broad zoning without significant contrast, but have straight and, occasionally, weak concentric oscillatory zoning consistent with an igneous origin (Fig. 7E). SHRIMP U-Pb analyses of these zircons cluster on concordia and yield a weighted average, for 18 spot determinations, of 1008 ± 4 Ma (Fig. 7F; $\pm 2\sigma$, MSWD = 1.13). We interpret this age to represent a precise estimate of the age of emplacement of the Lake Tiorati diorite body. Because this pluton is elsewhere deformed in a dextral, strike-slip, shear zone, this age provides an upper limit to strike-slip shearing on that zone.

Ar/Ar thermochronology was performed on samples of biotite and amphibole from both the western Hudson Highlands and the Reservoir Fault, NJ (Gates et al., 1999) (Fig. 2). The samples in the Hudson Highlands are from a mineralized zone within a dextral shear zone. The regional metamorphism was at such high temperature that individual events cannot be discerned and only slow regional cooling is observed in most cases. Hornblende yields consistent ages of 924–915

Table 1
Shrimp II U-Th-Pb data for hudson highlands zircons

Spot	Loc ^a	U (ppm)	Th (ppm)	Th/U	Pb*	²⁰⁶ Pb/ ²⁰⁴ Pb	²⁰⁷ Pb/ ²³⁵ U ± 1σ ^b	²⁰⁶ Pb/ ²³⁸ U ± 1σ ^b	²⁰⁷ Pb/ ²⁰⁶ Pb ± 1σ ^b	²⁰⁷ Pb/ ²⁰⁶ Pb age ± 1σ ^b (Ma)	Conc.
<i>G5 Semi-pelitic gneiss</i>											
13.2	c	172	19	0.112	63	138,313	6.3869 ± 0.1369	0.36795 ± 0.00571	0.12589 ± 0.00163	2041.4 ± 23.1	98.9
13.1	c	100	21	0.213	40	100,000	6.7980 ± 0.1157	0.39593 ± 0.00531	0.12453 ± 0.00111	2022.1 ± 15.9	106.3
14.1	c	369	183	0.513	105	48,146	3.3872 ± 0.0425	0.26369 ± 0.00297	0.09316 ± 0.00040	1491.2 ± 8.1	101.2
29.1	c	1646	606	0.380	385	11,714	2.7098 ± 0.0848	0.22601 ± 0.00576	0.08696 ± 0.00133	1359.6 ± 29.7	96.6
24.1	c	1130	291	0.266	254	100,000	2.6598 ± 0.0678	0.22368 ± 0.00518	0.08624 ± 0.00070	1343.7 ± 15.9	96.8
17.1	c	491	208	0.437	124	81,169	2.8501 ± 0.0325	0.24022 ± 0.00249	0.08605 ± 0.00031	1339.3 ± 7.1	103.6
28.1	c	1263	412	0.337	304	100,000	2.7922 ± 0.0700	0.23553 ± 0.00544	0.08598 ± 0.00062	1337.7 ± 14.1	101.9
18.1	m	168	60	0.367	40	255,754	2.7532 ± 0.0334	0.23419 ± 0.00249	0.08527 ± 0.00039	1321.6 ± 9.0	102.6
15.1	c	259	113	0.453	63	100,000	2.7103 ± 0.0344	0.23059 ± 0.00249	0.08525 ± 0.00046	1321.2 ± 10.5	101.2
36.1	c	975	852	0.902	268	13,464	2.8030 ± 0.0708	0.23853 ± 0.00563	0.08523 ± 0.00055	1320.7 ± 12.6	104.4
26.1	c	1156	616	0.550	280	16,250	2.6390 ± 0.0673	0.22666 ± 0.00527	0.08444 ± 0.00067	1302.8 ± 15.6	101.1
22.1	m	143	35	0.254	30	9851	2.4153 ± 0.0315	0.21162 ± 0.00223	0.08278 ± 0.00054	1264.0 ± 12.7	97.9
2.1	c	103	32	0.318	21	33,591	2.1911 ± 0.0357	0.19609 ± 0.00228	0.08104 ± 0.00082	1222.5 ± 19.9	94.4
16.1	c	269	23	0.090	54	389,105	2.3574 ± 0.0280	0.21172 ± 0.00227	0.08075 ± 0.00032	1215.5 ± 7.8	101.8
37.1	r	589	3	0.005	111	8186	2.2204 ± 0.0644	0.20232 ± 0.00487	0.07960 ± 0.00107	1187.0 ± 26.8	100.1
3.2	c	535	5	0.009	99	6328	2.1578 ± 0.0606	0.19789 ± 0.00482	0.07908 ± 0.00089	1174.2 ± 22.4	99.1
31.1	c	3187	19	0.006	546	37,679	1.9330 ± 0.0526	0.18497 ± 0.00449	0.07579 ± 0.00073	1089.6 ± 19.4	100.4
25.2	r	2140	14	0.007	341	21,805	1.7909 ± 0.0445	0.17234 ± 0.00403	0.07537 ± 0.00045	1078.3 ± 12.1	95.1
34.1	r	2298	61	0.027	375	35,625	1.7899 ± 0.0687	0.17538 ± 0.00527	0.07402 ± 0.00151	1042.0 ± 41.7	100.0
27.1	r	2277	36	0.016	372	15,855	1.7924 ± 0.0536	0.17644 ± 0.00454	0.07368 ± 0.00091	1032.6 ± 25.2	101.4
30.1	c	2595	54	0.021	419	17,734	1.7648 ± 0.0690	0.17377 ± 0.00529	0.07366 ± 0.00155	1032.1 ± 43.0	100.1
4.1	e	2389	38	0.017	387	338,983	1.7748 ± 0.0187	0.17484 ± 0.00177	0.07362 ± 0.00014	1031.1 ± 3.8	100.7
3.1	m	2802	119	0.044	472	357,143	1.8290 ± 0.0192	0.18029 ± 0.00182	0.07358 ± 0.00013	1029.9 ± 3.6	103.8
6.1	m	1292	27	0.021	207	226,244	1.7356 ± 0.0190	0.17241 ± 0.00174	0.07301 ± 0.00023	1014.3 ± 6.3	101.1
12.1	m	796	28	0.036	125	111,732	1.6965 ± 0.0180	0.16866 ± 0.00172	0.07295 ± 0.00015	1012.6 ± 4.1	99.2
5.1	e	1811	45	0.026	293	126,582	1.7514 ± 0.0181	0.17426 ± 0.00175	0.07289 ± 0.00011	1011.0 ± 3.1	102.4
21.1	m	1573	53	0.035	248	100,000	1.6978 ± 0.0184	0.16926 ± 0.00172	0.07275 ± 0.00020	1007.0 ± 5.5	100.1
19.1	r	2159	26	0.013	345	74,239	1.7319 ± 0.0182	0.17273 ± 0.00174	0.07272 ± 0.00014	1006.2 ± 3.9	102.1
23.1	c	1173	51	0.045	183	239,234	1.6737 ± 0.0176	0.16708 ± 0.00168	0.07265 ± 0.00015	1004.3 ± 4.3	99.2
8.1	m	718	22	0.032	113	95,694	1.6929 ± 0.0191	0.16906 ± 0.00172	0.07263 ± 0.00028	1003.5 ± 7.8	100.3
10.1	m	719	31	0.044	114	188,324	1.6929 ± 0.0192	0.16969 ± 0.00174	0.07235 ± 0.00027	995.9 ± 7.6	101.5

Table 1 (continued)

Spot	Loc ^a	U (ppm)	Th (ppm)	Th/U	Pb*	²⁰⁶ Pb/ ²⁰⁴ Pb	²⁰⁷ Pb/ ²³⁵ U ± 1σ ^b	²⁰⁶ Pb/ ²³⁸ U ± 1σ ^b	²⁰⁷ Pb/ ²⁰⁶ Pb ± 1σ ^b	²⁰⁷ Pb/ ²⁰⁶ Pb age ± 1σ ^b (Ma)	Conc.
11.1	e	817	23	0.030	129	196,850	1.6889 ± 0.0188	0.16930 ± 0.00173	0.07235 ± 0.00024	995.8 ± 6.8	101.3
9.1	c	1041	29	0.029	162	111,483	1.6686 ± 0.0189	0.16763 ± 0.00173	0.07219 ± 0.00026	991.4 ± 7.4	100.8
20.1	r	782	45	0.060	125	49,383	1.6942 ± 0.0217	0.17027 ± 0.00173	0.07217 ± 0.00048	990.7 ± 13.5	102.3
7.1	e	753	40	0.054	115	520,833	1.6315 ± 0.0181	0.16397 ± 0.00167	0.07216 ± 0.00024	990.6 ± 6.8	98.8
<i>G2 Quartzofeldspathic gneiss</i>											
19.2	m	281	130	0.480	61	100,000	2.3001 ± 0.0296	0.20458 ± 0.00214	0.08154 ± 0.00051	1234.6 ± 12.4	97.2
23.2	r	702	268	0.394	152	75,131	2.3412 ± 0.0259	0.20890 ± 0.00213	0.08128 ± 0.00026	1228.3 ± 6.3	99.6
10.1	m	281	122	0.450	59	100,000	2.2566 ± 0.0272	0.20157 ± 0.00209	0.08119 ± 0.00040	1226.1 ± 9.8	96.5
23.1	m	307	140	0.470	65	100,000	2.2349 ± 0.0353	0.20025 ± 0.00240	0.08095 ± 0.00072	1220.1 ± 17.6	96.4
19.1	r	1107	393	0.367	232	221,239	2.2793 ± 0.0251	0.20469 ± 0.00208	0.08076 ± 0.00026	1215.6 ± 6.2	98.8
13.1	c	150	80	0.550	33	100,000	2.2543 ± 0.0287	0.20322 ± 0.00224	0.08045 ± 0.00041	1208.1 ± 10.1	98.7
2.1	m	207	100	0.500	44	100,000	2.2353 ± 0.0279	0.20168 ± 0.00208	0.08039 ± 0.00047	1206.5 ± 11.6	98.2
22.1	c	85	44	0.531	19	59,488	2.2950 ± 0.0383	0.20725 ± 0.00240	0.08031 ± 0.00085	1204.7 ± 21.1	100.8
6.1	r	477	189	0.409	101	100,000	2.2576 ± 0.0271	0.20411 ± 0.00212	0.08022 ± 0.00039	1202.4 ± 9.6	99.6
21.1	m	352	145	0.427	76	36,711	2.2905 ± 0.0350	0.20758 ± 0.00215	0.08003 ± 0.00080	1197.6 ± 19.9	101.5
3.1	e	1719	525	0.316	360	689,655	2.2845 ± 0.0353	0.20722 ± 0.00251	0.07996 ± 0.00065	1195.9 ± 16.2	101.5
2.2	r	719	229	0.330	149	100,000	2.2510 ± 0.0270	0.20421 ± 0.00217	0.07994 ± 0.00035	1195.6 ± 8.7	100.2
9.2	r	495	192	0.402	105	100,000	2.2548 ± 0.0254	0.20474 ± 0.00212	0.07987 ± 0.00027	1193.9 ± 6.6	100.6
1.2	c	66	35	0.546	14	111,857	2.2036 ± 0.0363	0.20019 ± 0.00259	0.07984 ± 0.00070	1193.0 ± 17.4	98.6
5.1	m	212	97	0.472	45	100,000	2.1913 ± 0.0415	0.19992 ± 0.00274	0.07950 ± 0.00091	1184.5 ± 22.8	99.2
16.1	e	922	310	0.348	186	13,483	2.1568 ± 0.0242	0.19746 ± 0.00203	0.07922 ± 0.00028	1177.7 ± 6.9	98.6
17.1	e	782	293	0.387	167	95,238	2.2626 ± 0.0254	0.20740 ± 0.00213	0.07912 ± 0.00028	1175.2 ± 7.0	103.4
24.1	c?	390	197	0.523	85	100,000	2.2258 ± 0.0281	0.20419 ± 0.00234	0.07906 ± 0.00032	1173.6 ± 8.0	102.1
8.1	c	90	59	0.675	20	8982	2.1489 ± 0.0389	0.19777 ± 0.00246	0.07881 ± 0.00092	1167.3 ± 23.3	99.7
4.1	e	1901	379	0.206	373	93,197	2.1689 ± 0.0223	0.19963 ± 0.00201	0.07880 ± 0.00009	1167.1 ± 2.3	100.5
1.1	m	297	134	0.467	64	100,000	2.2219 ± 0.0269	0.20505 ± 0.00218	0.07859 ± 0.00036	1161.8 ± 9.1	103.5
14.1	r	1390	386	0.287	283	160,000	2.2045 ± 0.0295	0.20375 ± 0.00230	0.07847 ± 0.00047	1158.8 ± 11.8	103.2
7.2	r	1527	148	0.100	241	21,177	1.6833 ± 0.0473	0.16622 ± 0.00422	0.07345 ± 0.00068	1026.3 ± 19.0	96.6
25.1	r	1712	73	0.044	289	40,096	1.8225 ± 0.0527	0.18064 ± 0.00472	0.07317 ± 0.00069	1018.7 ± 19.3	105.1
15.1	r	1458	169	0.120	241	100,000	1.7370 ± 0.0194	0.17295 ± 0.00176	0.07284 ± 0.00026	1009.6 ± 7.2	101.9

(continued on next page)

Table 1 (continued)

Spot	Loc ^a	U (ppm)	Th (ppm)	Th/U	Pb*	²⁰⁶ Pb/ ²⁰⁴ Pb	²⁰⁷ Pb/ ²³⁵ U ± 1σ ^b	²⁰⁶ Pb/ ²³⁸ U ± 1σ ^b	²⁰⁷ Pb/ ²⁰⁶ Pb ± 1σ ^b	²⁰⁷ Pb/ ²⁰⁶ Pb age ± 1σ ^b (Ma)	Conc.
<i>G1 Lake Tiorati diorite</i>											
10.1	if	366	183	0.517	66	100,000	1.7145 ± 0.0230	0.16979 ± 0.00178	0.07323 ± 0.00053	1020.5 ± 14.7	99.1
5.1	if	702	117	0.173	118	100,000	1.7444 ± 0.0203	0.17297 ± 0.00176	0.07314 ± 0.00033	1017.8 ± 9.2	101.0
19.1	if	325	84	0.267	55	100,000	1.7049 ± 0.0219	0.16916 ± 0.00188	0.07310 ± 0.00038	1016.6 ± 10.5	99.1
6.1	if	691	136	0.204	116	67,476	1.7319 ± 0.0185	0.17204 ± 0.00177	0.07301 ± 0.00013	1014.3 ± 3.7	100.9
18.1	if	330	213	0.668	60	83,126	1.6685 ± 0.0208	0.16576 ± 0.00169	0.07301 ± 0.00044	1014.1 ± 12.3	97.5
8.2	if	747	364	0.503	135	271,739	1.7359 ± 0.0193	0.17249 ± 0.00175	0.07299 ± 0.00025	1013.6 ± 6.9	101.2
11.1	if	529	316	0.617	98	20,488	1.7115 ± 0.0205	0.17021 ± 0.00174	0.07293 ± 0.00038	1011.9 ± 10.5	100.1
16.1	if	654	694	1.097	137	100,000	1.7281 ± 0.0198	0.17225 ± 0.00178	0.07276 ± 0.00028	1007.3 ± 7.8	101.7
2.1	if	624	241	0.399	110	131,234	1.7190 ± 0.0201	0.17135 ± 0.00180	0.07276 ± 0.00029	1007.2 ± 8.1	101.2
14.1	if	397	246	0.639	73	2147	1.6748 ± 0.0254	0.16727 ± 0.00174	0.07262 ± 0.00071	1003.4 ± 20.1	99.4
13.1	if	312	70	0.233	52	66,138	1.6991 ± 0.0222	0.16970 ± 0.00174	0.07262 ± 0.00050	1003.3 ± 14.1	100.7
8.1	if	356	218	0.632	65	36,819	1.6658 ± 0.0193	0.16657 ± 0.00175	0.07253 ± 0.00027	1000.9 ± 7.6	99.2
9.1	if	416	136	0.338	70	42,319	1.6654 ± 0.0205	0.16662 ± 0.00171	0.07250 ± 0.00041	999.9 ± 11.6	99.4
7.1	if	191	75	0.407	33	19,131	1.6581 ± 0.0242	0.16607 ± 0.00181	0.07241 ± 0.00061	997.6 ± 17.3	99.3
3.1	if	486	190	0.404	81	205,339	1.6218 ± 0.0196	0.16281 ± 0.00168	0.07224 ± 0.00037	992.8 ± 10.3	97.9
4.1	if	478	287	0.620	86	45,106	1.6631 ± 0.0192	0.16699 ± 0.00171	0.07223 ± 0.00030	992.5 ± 8.5	100.3
12.1	if	267	71	0.273	45	32,992	1.7024 ± 0.0244	0.17122 ± 0.00184	0.07211 ± 0.00059	989.1 ± 16.8	103.0
17.1	if	455	327	0.744	87	37,836	1.6952 ± 0.0207	0.17081 ± 0.00175	0.07198 ± 0.00040	985.3 ± 11.3	103.2

Corrections for common Pb made using measured ²⁰⁴Pb. Data were acquired using either a larger (~29×35 micron) primary O⁻ beam with a strength of approximately 15nA, or with a smaller Kohler aperture creating a primary beam with an analytical spot diameter of ~10×13 microns and a current of approximately 1.0–1.5 nA. Calibration of Pb/U ratios was referenced to GSC zircon standard BR266 (559 Ma). Pb*—radiogenic Pb.

^a Location of spot analysis: c = core, m = mantle, r = rim, e = equant and homogeneous, if = fragment of magmatic grain showing simple igneous zoning (igneous fragment).

^b All errors on ratios and ages reported at 1σ level of uncertainty, absolute.

^c Percent concordant.

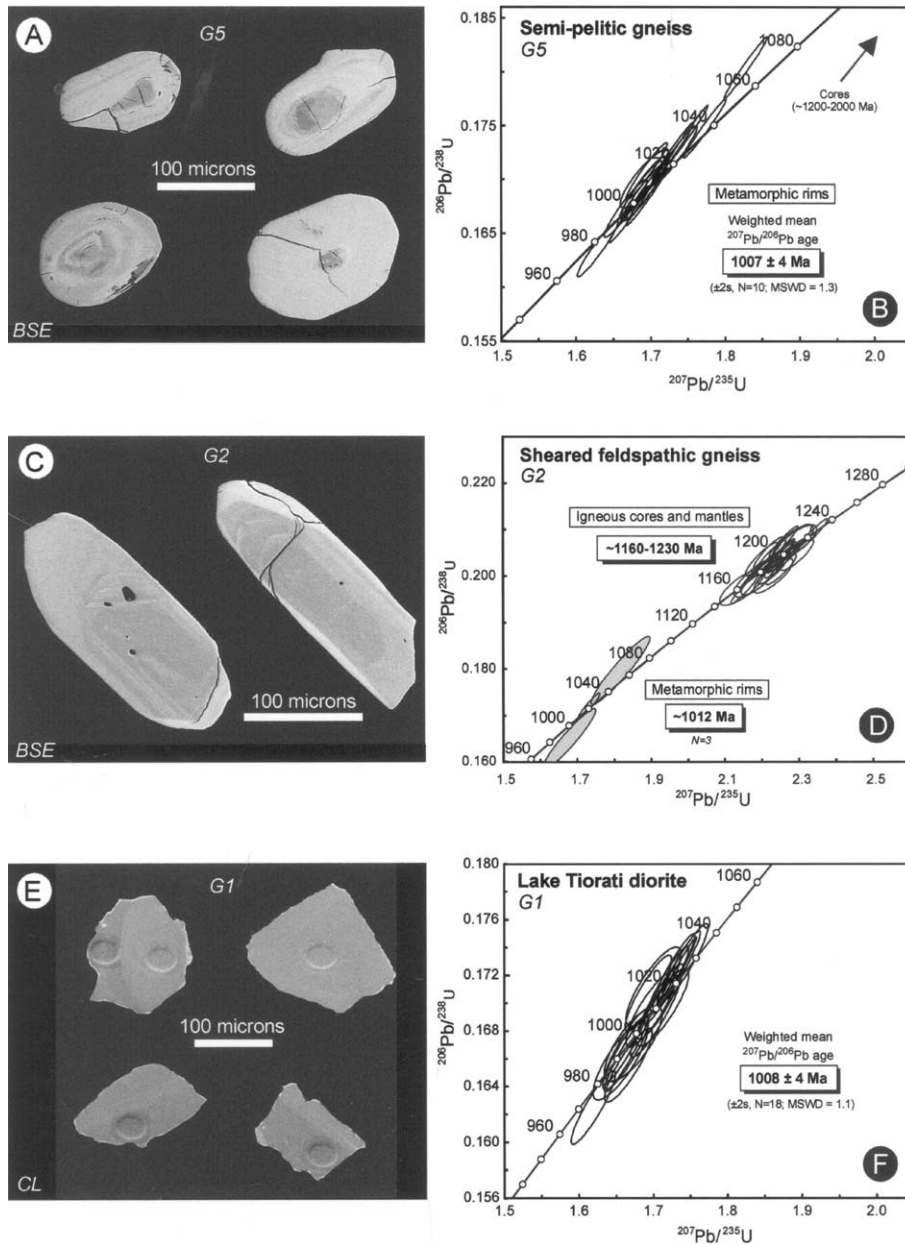


Fig. 7. Scanning electron microscopy images of representative zircons and corresponding concordia plots for U-Pb SHRIMP analyses from Hudson Highlands rocks. See Fig. 2 for sample localities. (A) and (B) Sample G5, from semi-pelitic gneiss of metasedimentary origin. Backscattered electron (BSE) image. Note small detrital cores and thick metamorphic rims. Concordia plot shows data from metamorphic rims only. (C) and (D) Sample G2, from quartzofeldspathic gneiss of metavolcanic origin. Note broad, zoned magmatic cores and thin, bright unzoned metamorphic rims in BSE image. Unfilled concordia ellipses represent zoned igneous cores and mantles. Shaded ellipses are three high-U, low Th/U unzoned metamorphic rims yielding an average $^{207}\text{Pb}/^{206}\text{Pb}$ age of ~ 1012 Ma. (E) and (F) Sample G1, from sheared Lake Tiorati diorite. Note broad, straight igneous zoning evident in cathodoluminescence (CL) image. Circular depressions in CL image are SHRIMP analysis pits. All ellipses shown with 1-sigma errors.

Ma, whereas biotite yields 795–820 Ma. However, neoblastic hastingsitic amphibole from low-temperature cataclasite with consistent dextral offset from the Reservoir Fault, NJ (Gates, 1995) yields 876 Ma. The Reservoir Fault is regionally continuous from the field area in the western Hudson Highlands to the sampled location in the New Jersey Highlands.

Geochronologic studies in the Adirondack Highlands constrain the timing of compressional deformation, peak metamorphic conditions, and late syn- to post-tectonic intrusives to 1090–1030 Ma after the intrusion of vast volumes of AMCG plutonic rocks from 1160 to 1100 Ma (McLelland et al., 1988, 1996). Although displacement along the MRPSZ may have been active during the time of regional high-grade metamorphism (Ottawan orogeny), sinistral transpression along the PLSZ clearly post-dates, and is superimposed on, compressional orogenesis and granulite-facies mineral assemblages. A lower limit can be placed on transpression in the southern Adirondacks, at least locally, where an undeformed, 950 Ma, leucogranitic dike swarm intrudes strongly lineated gneiss (McLelland et al., 1996).

5.1. Post-Ottawan events in the Adirondacks

Recently published argon data ($^{40}\text{Ar}/^{39}\text{Ar}$) from biotite in samples collected near the Carthage-Colton shear zone in the Adirondacks suggest extensional movement occurred at 950–920 Ma (Streepey et al., 2000), well after the cessation of compression at 1030 Ma in the Adirondacks (McLelland et al., 1996). Given the nearly 100 Ma difference in timing between compression and extension, Streepey et al. (2000) suggested that movement on the Carthage-Colton shear zone was not related to orogenic collapse, but to an undefined, enigmatic extensional event in eastern Laurentia.

Interpretations suggest that the Adirondacks cooled at a rate of 1–2 °C/Ma during a period of at least 100 Ma at this time (Mezger et al., 1993). The significance of extended periods of slow cooling is not yet fully understood; however, strike-slip deformation related to orogen parallel deformation after 1050 Ma provides a plausible mechanism for the slow uplift of the region over an extended timeframe. In the Adirondack Highlands, cooling rates are thought to have increased to 4 °C/Ma at ca. 950 Ma (Streepey et al., 2000). The scenario proposed here, late strike-slip modification of Ottawan compressional structures in a large syntaxis, provides a realistic time frame for Rodinia assembly, a plausible mechanism for extension, and an explanation of otherwise enigmatic P-T-t paths.

6. Tectonic model

The synchronous, broad, crossing zones of deformation with opposing shear sense identified in the Adirondacks and Reading Prong appear to represent a crustal-scale conjugate shear system (Fig. 8). Clearly, the limitations on this interpretation are the great distance between these two Grenville terranes that is covered by Paleozoic sedimentary rock and the potential modifications to the geometrical relations as the result of Paleozoic orogenesis among others. Nonetheless, the similarity in timing and character and evidence of numerous outcrop-scale, conjugate, shear-zone relations with similar orientations in both areas render the model plausible. Although the Adirondacks and Hudson Highlands are only a small portion of the Grenville Province, and

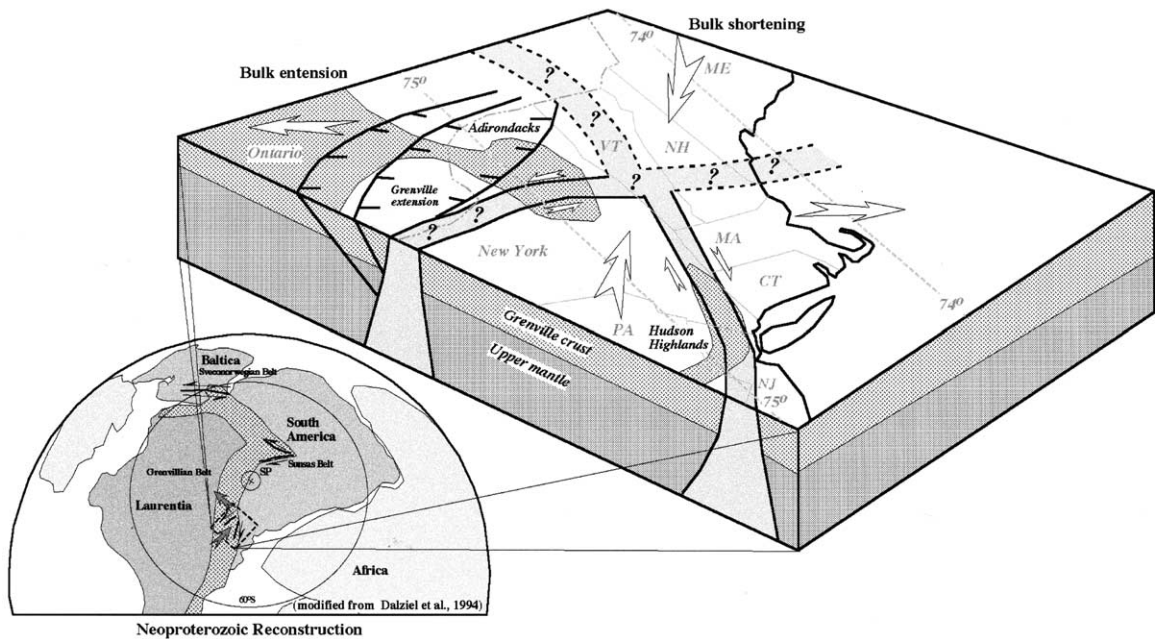


Fig. 8. Tectonic model for the Grenville conjugate shear system showing the relations among dextral, sinistral and extensional faulting in NY state. The inset shows the Neoproterozoic reconstruction of Rodinia and location of the proposed conjugate shear system within the Grenville orogen (modified from Dalziel et al., 1994).

thus extrapolation of this model to the orogen scale is speculative, oblique convergence and orogen-parallel transpression accompanying orogenesis of “Ottawan” age has been noted in other areas including the Central Gneiss Belt in Ontario (Gower, 1992), Baltica (Stephens et al., 1996; Park, 1992), and South America (Sadowski and Bettencourt, 1996). Thus the findings synthesized here may have significant tectonic implications for the final assembly of Rodinia over a broad area.

Supporting evidence for the model comes from paleomagnetic polar wander paths for both North America and Baltica. They show a pronounced 90° bend at about ca. 1020 Ma (Fig. 9) which is consistent with an abrupt change in plate motion, perhaps in response to a shift from convergence to strike-slip motion (Bylund, 1992; Park and Gower, 1996).

Even if plate convergence was purely orthogonal, considerable strike-slip faulting and horizontal-escape tectonism due to plate-margin geometry is possible. The Himalayan stress field is related to the shape of the Indian subcontinent (rigid indenter of Tapponnier and Molnar, 1976) and resulted in the lateral escape of crustal blocks in southeast Asia along major transcurrent zones. In contrast, the Himalayan contractional structures (thrusts and fold nappes) are of limited areal extent. Recent work has shown that the stress field in the crust is reflected in the subcontinental mantle (Holt, 2000). The fast polarization direction of split shear waves beneath the Adirondacks has been shown to be E–W (Barruol et al., 1997), parallel to the east-west structural fabric of the south-central Adirondacks and earthquake first motions (Dawers and Seeber, 1991). This east-west trend truncates the prevalent northeast-trend of both the Grenville and Appalachian orogen in eastern North America (Barruol et al., 1997). Because the Hudson

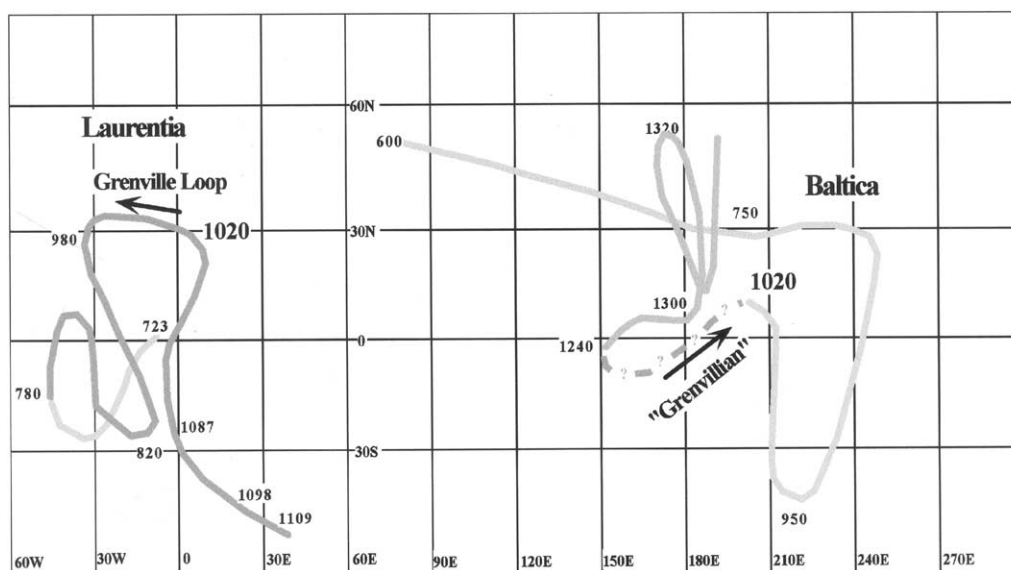


Fig. 9. Polar wandering paths for Laurentia and Baltica during the middle and late Proterozoic (modified from Bylund, 1992; and Park and Gower, 1996).

Highlands are outboard of the Adirondacks, they were positioned near the margin of Laurentia or originated as part of the overriding South American (Dalziel et al., 1994) continent. The recognition of strike-slip faulting and transpression in the Grenville core may record the escape of tectonic elements (Gates, 1995) and enhances analogs drawn with the Himalayas and models based on indentation tectonics (Hoffman, 1992).

Based upon existing age constraints, this conjugate shear system was active in the core of the Ottawa Orogen during and subsequent to peak metamorphic conditions and within the range of ca. 1008–876 Ma. Relative to modern geographic coordinates, the Grenville strike-slip shear zones yield bulk-extension and bulk-compression directions of west-northwest and east-northeast respectively. These strain axes are consistent with compression directions deduced from en echelon transpressional folds in the Hudson Highlands and the en-echelon domes on the central Adirondacks (Chiarenzelli et al., 2000). This bulk strain analysis assumes that bulk rotation of the Hudson Highlands relative to the Adirondacks during Paleozoic Appalachian tectonic events (Taconic, Acadian, Alleghanian orogenies) and Mesozoic extension was minimal. The assumption is reasonable because (1) there is no post-Precambrian penetrative deformation in the western Hudson Highlands and (2) the major folds and faults in the surrounding Paleozoic strata are essentially parallel to those in the crystalline rocks indicating similar strain axes and minimal rotation.

The extensional deformation identified in the northwestern Adirondacks can be explained using the conjugate model with the interpreted bulk-strain directions (Fig. 8). The Grenville Province north of the Adirondack Lowlands contains numerous Proterozoic normal faults and shear zones with an overall northwest-southeast extension direction (Streepey et al., 2000), and published age data suggest that these normal faults were active as much as 100 Ma after peak metamorphic conditions in the Adirondack Highlands. The conjugate shear model presented here is consistent with the orientation, timing, and location of these later extensional faults such as the Carthage–

Colton mylonite zone (separating the amphibolite facies Adirondack Lowlands from the Highlands) and extension in the Central Metasedimentary Belt in Ontario (van der Pluijm and Carlson, 1989).

Gates (1995) proposed that eastern Laurentia underwent escape tectonism along major faults as a result of a second Grenville collision somewhere between the present New England and Labrador. This model must be reconsidered in light of the new data. The early Himalayan-type collision that formed the westward-directed fold nappes and granulite-facies metamorphism is present throughout the Grenville orogen. The transcurrent-transpressional deformation post-dates it. This deformation could still have resulted from a second collision, but it could also have been the second phase of a single event like the Himalayas, where the escape tectonic features overprint the earlier contractional features. The extensive sinistral shearing in the Adirondacks equals or may even exceed the exposed dextral shearing in the Hudson Highlands. However, strike-slip deformation has yet to be identified in the Blue Ridge Province in the southern Appalachians. Therefore, the marked predominance of one conjugate fault set over the other as in the Himalayas does not appear to be the case in the study area. Instead, the distribution of the conjugate faulting appears relatively balanced. This situation may have resulted from the location of the area directly in front of the “indenter” or the lack of a “free face” (Tapponnier et al., 1982) that characterizes the Himalayan geometry. An uneven, leading, South American margin with promontories that impinged on the equally irregular Laurentian margin could have produced local syntaxes with relatively balanced conjugate transcurrent faulting. There are several potential syntaxes along the Grenville margin including the Sunsas Belt of Brazil (Sadowski and Bettencourt, 1996).

7. Conclusions

Comparison of major Proterozoic strike-slip shear zones in the Reading Prong (PA, NJ, NY) and the Adirondacks (NY) indicates that there may have been a Himalayan-type syntaxis developed in eastern Laurentia during the final assembly of Rodinia. The band of dextral shear zones in the Hudson Highlands of New York has been expanded to 35-km width with new mapping. Ages of movement are constrained between ca. 1008 and 876 Ma with new isotopic dating using SHRIMP. Two newly described, major, sinistral, strike-slip shear zones (Piseco Lake shear zone and Moose River plain shear zone) form a 60-km wide band across the southern Adirondacks. Ages of movement are roughly constrained between ca. 1050 and 950 Ma. These data and numerous pieces of supporting evidence, ranging from paleomagnetic data to analogs elsewhere along the Grenville orogen, support a conjugate strike-slip, and thus, a syntaxis model. This syntaxis may elucidate yet unobserved processes that are occurring in the roots of Himalayas.

Acknowledgements

Funding for mapping in the Hudson Highlands was through a STATEMAP project with the New York State Geological Survey and US Geological Survey. Mapping in Pennsylvania was

funded by the Pennsylvania Geological Survey. Analytical work was funded through grants from the Harriman and Perkins Family Foundations and the J.M. Kaplan Fund. Funding for mapping in the Adirondacks was through The State University of New York at Oswego faculty enhancement and CISCA grants, and UUP grants. R. Stern is thanked for providing access to the Geological Survey of Canada's Ion Microprobe (SHRIMP II) Laboratory in Ottawa. Discussions with J. McLelland, R. Fakundiny, P. Whitney, M. Gorrington, R. Volkert, W. Romey, R. Berman, L. Aspler, W. Orndorff, T. Marsh, and J. Valley, and reviews by P. Whitney, J. McClelland, G. Walsh and F. Ettensohn are gratefully acknowledged.

References

- Baer, A.J., 1977. The Grenville province as a shear zone. *Nature* 267, 337–338.
- Barruol, G., Silver, P., Vauchez, A., 1997. Seismic anisotropy in the eastern US: Deep structure of a complex continental margin. *Journal of Geophysical Research* 102, 8329–8348.
- Bylund, G., 1992. Palaeomagnetism of mafic dykes and the Protogine Zone, southern Sweden. *Tectonophysics* 201, 149–167.
- Chiarenzelli, J., Valentino, D., Gates, A., 2000. Sinistral transpression in the Adirondack Highlands during the Ottawa Orogeny: strike-slip faulting in the deep Grenvillian crust: Abstract Millennium Geoscience Summit GeoCanada 2000. Calgary, Alberta.
- Dalziel, I.W.D., Salada, L.H.D., Gahagan, L.M., 1994. Paleozoic Laurentian-Gondwana interaction and the origin of the Appalachian-Andean mountain system. *Geological Society of America Bulletin* 106, 243–252.
- Dawers, N., Seeber, L., 1991. Intraplate faults revealed in the crystalline bedrock in the 1983 Goodnow and 1985 Ardsley epicentral areas, New York. *Tectonophysics* 186, 115–131.
- DeWaard, D., Romey, W., 1969. Petrogenetic relationships in the anorthosite-charnockite series of the Snowy Mountain dome, south central Adirondacks. In: Isachsen, Y.W. (Ed.), *Origin of anorthosites and related rocks* 18. New York State Science, Service Memoir, NY, pp. 307–315.
- Dewey, J., Burke, K., 1973. Tibetan, Variscan and Precambrian basement reactivation: products of continental collision. *Journal of Geology* 81, 683–692.
- Gates, A., 1995. Middle Proterozoic dextral strike-slip event in the Central Appalachians: Evidence from the reservoir Fault, NJ. *Journal of Geodynamics* 19, 195–212.
- Gates, A.E., 1999. Early compression and late dextral transpression within the Grenvillian Event of the Hudson Highlands, NY, USA. In: Sinha, A.K. (Ed.), *Basement Tectonics 13*; Dordrecht. Kluwer Academic Publishers, The Netherlands, pp. 85–98.
- Gates, A.E., Costa, R.E., 1998. Multiple reactivations of rigid basement block margins: Examples in the northern Reading Prong, USA. In: Gilbert, M.C., Hogan, J.P. (Eds.), *Basement Tectonics 12: Central North America and Other Regions*; Dordrecht. Kluwer Academic Publishers, The Netherlands, pp. 123–153.
- Gates, A.E., Valentino, D.W., Krol, M.A., 1999. The Grenville Province in the western Hudson Highlands, southern New York. *Friends of the Grenville Field Conference Guidebook*, Montreal, CN.
- Glennie, J.S., 1973. Stratigraphy, structure, and petrology of the Piseco Dome area, Piseco Lake 15' quadrangle, southern Adirondack Mountains, New York [Ph.D. thesis]. Syracuse, New York, Syracuse University, 45 pp.
- Gower, R., 1992. Nappe emplacement direction in the Central Gneiss Belt, Grenville Province Ontario, Canada: evidence for oblique collision. *Precambrian Research* 59, 73–94.
- Hamilton, M.A., McLelland, J., Selleck, B., in press, SHRIMP U-Pb zircon geochronology of the anorthosite-mangerite-charnockite-granite (AMCG) suite, Adirondack Mountains, New York: ages of emplacement and metamorphism: In Tollo, R.P., Corriveau, L., McLelland, J., Bartholomew, M.J., (eds.), *Proterozoic Tectonic Evolution of the Grenville Orogen in North America*. Geological Society of America Memoir.
- Hoffman, P., 1992. Global Grenville kinematics and fusion of the Neoproterozoic Supercontinent Rodinia. *Geological Association of Canada Program with Abstracts* 17, 49.

- Holt, W., 2000. Correlated crust and mantle strain fields in Tibet. *Geology* 28, 67–70.
- Lister, G.S., Snoke, A.W., 1984. S-C mylonites. *Journal Structural Geology* 6, 617–638.
- McLelland, J., 1984. Origin of ribbon lineation within the southern Adirondacks, USA. *Journal of Structural Geology* 6, 147–157.
- McLelland, J., Isachsen, Y., 1986. Synthesis of geology of the Adirondack Mountains, New York, and their tectonic setting within the southwestern Grenville Province, In: Moore, J.M., Davidson, A., Baer, A., (Eds.), *The Grenville Province*. Geological Association of Canada Special Paper 31, p. 75–94.
- McLelland, J., Chiarenzelli, J., Whitney, P., Isachsen, Y., 1988. U-Pb zircon geochronology of the Adirondack Mountains and implications for their geologic evolution. *Geology* 16, 920–924.
- McLelland, J., Daly, S., McLelland, J., 1996. The Grenville orogenic cycle (ca. 1350–1000 Ma): an Adirondack perspective. *Tectonophysics* 265, 1–28.
- McLelland, J., Hamilton, M., Selleck, B., McLelland, J., Walker, D., Orrell, S., 2001. Zircon U-Pb geochronology of the Ottawa Orogeny, Adirondack Highlands, New York; regional and tectonic implications. *Precambrian Research* 109, 39–72.
- Mezger, K., Essene, E.J., van der Pluijm, B.A., Halliday, A., 1993. N, U-Pb geochronology of the Grenville Orogen of Ontario and New York; constraints on ancient crustal tectonics. *Contributions to Mineralogy and Petrology* 114, 13–26.
- Mose, D.G., 1982. 1,300 million-year-old rocks in the Appalachians. *Geological Society of America Bulletin* 93, 391–399.
- Park, R., 1992. Plate kinematic history of Baltica during the Middle to Late Proterozoic: a model. *Geology* 20, 725–728.
- Park, J., Gower, C., 1996. Paleomagnetism of pre-Grenville mafic rocks from the southeast Grenville Province, Labrador: implications for the Grenville track. *Canadian Journal of Earth Sciences* 33, 746–756.
- Passchier, C.W., Simpson, C., 1986. Porphyroclast systems as kinematic indicators. *Journal of Structural Geology* 8, 831–843.
- Rivers, T., 1997. Lithotectonic elements of the Grenville Province: review and tectonic implications. *Precambrian Research* 86, 117–154.
- Sadowski, G., Bettencourt, J., 1996. Mesoproterozoic tectonic correlations between eastern Laurentia and the western border of the Amazon Craton. *Precambrian Research* 76, 213–227.
- Simpson, C., Schmid, S.M., 1983. An evaluation of criteria to deduce the sense of movement in sheared rock. *Geological Society America Bulletin* 94, 1281–1288.
- Stephens, M., Wahlgren, C.-H., Weijermars, R., Cruden, A., 1996. Left-lateral transpressive deformation and its tectonic implications, Sveconorwegian orogen, Baltic Shield, southwestern Sweden. *Precambrian Research* 79, 261–279.
- Stern, R.A., 1997. The GSC sensitive high resolution ion microprobe (SHRIMP): analytical techniques of zircon U-Th-Pb age determinations and performance evaluation: In *Radiogenic age and isotopic studies: Report 10*. Geological Survey of Canada, Current Research 1997-F, 1–31.
- Streepey, M.M., van der Pluijm, B.A., Essene, E.J., Hall, C.M., Magloughlin, J.F., 2000. Late Proterozoic (ca. 930 Ma) extension in eastern Laurentia. *Geological Society of America Bulletin* 112, 1522–1530.
- Tapponnier, P., Molnar, P., 1976. Slip-line field theory and large scale continental tectonics. *Nature* 264, 319–324.
- Tapponnier, P., Molnar, P., 1977. Rigid plastic indentation; the origin of syntaxis in the Himalayan Belt, Himalaya. *Sciences de la terre, Colloques Internationaux du Centre National de la Recherche Scientifique* 268, 431–432.
- Tapponnier, P., Peltzer, G., Le Bail, A.Y., Armijo, R., Cobbold, P., 1982. Propagating extrusion tectonics in Asia: New insights from simple experiments with plasticine. *Geology* 10, 614–616.
- van der Pluijm, B., Carlson, K., 1989. Extension in the Central metasedimentary Belt of the Ontario Grenville: Timing and tectonic significance. *Geology* 17, 161–164.
- Wasteneys, H., McLelland, J., Lumbers, S., 1999. Precise zircon geochronology in the Adirondack Lowlands and implications for revising plate tectonic models of the Central Metasedimentary Belt and Adirondack Mountains, Grenville Province, Ontario and New York. *Canadian Journal of Earth Sciences* 36, 967–984.
- Wiener, R.W., McLelland, J.M., Isachsen, Y.W., Hall, L.M., 1984. Stratigraphy and structural geology of the

- Adirondack Mountains, New York: Review and Synthesis, In: Bartholomew, M.J., (Ed.), *The Grenville Event in the Appalachians and Related Topics*, Geological Society of America Special Paper 194, 1–56.
- Windley, B., 1986. Comparative tectonics of the western Grenville and the western Himalaya, In: Moore, J.M., Davidson, A., Baer, A.J., (Eds.), *The Grenville Province*; Geological Association of Canada Special Paper, 31, 341–348.